Journal of Zhejiang University SCIENCE A
ISSN 1673-565X (Print); ISSN 1862-1775 (Online)
www.zju.edu.cn/jzus; www.springerlink.com
E-mail: jzus@zju.edu.cn

Resonant frequencies of a piezoelectric drum transducer*

Jiang-bo YUAN†, Tao XIE, Xiao-biao SHAN, Wei-shan CHEN

(*State Key Laboratory of Advanced Robot and System, Harbin Institute of Technology, Harbin 150001, China*)

†E-mail: yjb0420@126.com

Received Nov. 19, 2008; Revision accepted Dec. 12, 2008; Crosschecked July 8, 2009

Abstract: This paper presents a piezoelectric-metal structure called a drum transducer. An equation for calculating the resonance frequency of the drum transducer is obtained based on thin plate elastic theory of piezoelectric and metal material combined with the Rayleigh-Ritz method. The finite element method (FEM) was used to predict the excitation frequency of the drum transducer. To verify the theoretical analysis, the input impedance characteristic of the drum transducer was measured using an experimental method. The results obtained from theoretical analysis were in very good agreement with those from the FEM and experimental results. The effect of geometrical changes to the thick-walled steel ring of the drum transducer at the first resonance frequency is also described. The calculated results were found to be in good agreement with the FEM results. The results indicate that the first resonance frequency of the drum decreases with the increasing inner diameter of the thick-walled steel ring.

Key words: Piezoelectric, Drum transducer, Resonance frequency
doi:10.1631/jzus.A0820804 **Document code:** A **CLC number:** TM356

INTRODUCTION

In recent years, solid state devices using piezoelectric effects have drawn much attention both scientifically and technologically. Piezoelectric actuators, sensors, and transducers have been widely used in many electromechanical applications including active and passive vibration damping, ultrasonic motors, ultrasonic biomedical imaging, loudspeakers, accelerometers, resonators, acoustic sensors and energy harvesting (Uchino, 1999; Hao and Chen, 2006; Chen and Shi, 2007; Li *et al*., 2007; Wang *et al*., 2007). A novel piezoceramic-metal composite structure called the piezoelectric drum transducer was studied as an actuator by Sun *et al*.(2006; 2007). The drum transducer has a high piezoelectric charge coefficient, about twice as large as that of a cymbal actuator with the same ceramic material and comparable dimensions. It also has a very short response time and a high effective coupling coefficient. The use of wireless sensors and wearable electronics has grown steadily over the past few decades. Due to the limited lifetime of electrochemical batteries, many researchers have studied the concept of using piezoelectric material for energy generation (Cornwell *et al*., 2005; Kim *et al*., 2006; 2007; Mateu and Moll, 2005; 2007; Wang *et al*., 2007). Recent research on the use of drum transducers in energy harvesting was described by Wang *et al*.(2007). A power of 11 mW was generated under a prestress of 0.15 N and a cyclic stress of 0.7 N at the resonance frequency of the drum transducer (590 Hz) across an 18 kΩ resistor. The resonance frequency of the piezoelectric transducer is a crucial parameter for the piezoelectric actuator and energy harvesting device, and is proportional to the displacement amplification and the harvested power.

In this paper, an equation for calculating the resonance frequency of the drum transducer is obtained based on the thin plate elastic theory of piezoelectric and metal material combined with the Rayleigh-Ritz method. The finite element method (FEM) was used to analyze the vibration mode of the drum transducer. To verify the theoretical analysis, the input impedance characteristic of the drum transducer was measured using an experimental method. The effect of geometrical changes in the

* Project supported by the National Natural Science Foundation of China (No. 50875057), and the Natural Scientific Research Innovation Foundation in Harbin Institute of Technology, China (No. HIT.NSRIF.2008.50)

thick-walled steel ring of the drum transducer on the resonance frequencies is also described.

SAMPLE PREPARATION

Fig.1 shows a schematic diagram of the drum transducer. A short, thick-walled steel ring is sandwiched by two thin composite disks, fabricated from a brass disk bonded with a piezoelectric (PZT) disk, which serve as the driving units of the drum transducer (Sun *et al*., 2006; 2007; Wang *et al*., 2007). The piezoceramic disks of the composite disks have a diameter of d_3 and a thickness of $(t_3-t_2)/2$. The brass disks of the composite disks have a diameter of d_2 and a thickness of $(t_2-t_1)/2$, and the short, thick-walled steel ring has an inner diameter of d_1 and a depth of t_1. The diameters of the piezoceramic disks, brass disks and steel ring are much greater than their thicknesses.

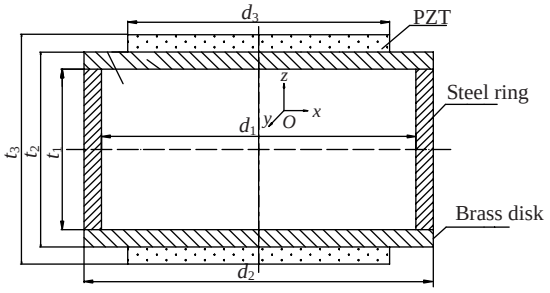

Fig.1 Schematic diagram of a drum transducer

THEORETICAL ANALYSIS

When an electric field, E, is applied in the thickness direction of the composite disks, the piezoceramic disks of the composite disks polarized in their thickness direction have a large diameter thickness ratio, and a large flexural deformation is produced. The induced radial strain of the ceramic disks causes a bending of the composite disks in the normal direction. The total generated strain energy of the drum transducer U will be generated and can be obtained as follows:

$$U=U_1+U_2+U_3, \tag{1}$$

where U_1 is the strain energy of the PZT and brass composite disk where $r\leq r_3$; U_2 is the strain energy of the brass ring where $r_3<r\leq r_2$; U_3 is the strain energy of the steel ring where $r_1\leq r\leq r_2$; r_1 is the inner radius of the steel ring, and r_2 and r_3 are the radii of the brass disk and PZT, respectively.

Based on g-type piezoelectric equations, the constitutive equations for a piezoelectric element are given (Liu *et al*., 2002):

$$T_1=\frac{1}{s_{11}(1-\sigma_3^2)}S_1+\frac{\sigma_3}{s_{11}(1-\sigma_3^2)}S_2-\frac{g_{31}}{s_{11}(1-\sigma_3^2)}D_3, \tag{2a}$$

$$T_2=\frac{\sigma_3}{s_{11}(1-\sigma_3^2)}S_1+\frac{1}{s_{11}(1-\sigma_3^2)}S_2-\frac{g_{31}}{s_{11}(1-\sigma_3^2)}D_3, \tag{2b}$$

$$E_3=-\frac{g_{31}}{s_{11}(1-\sigma_3)}S_1-\frac{g_{31}}{s_{11}(1-\sigma_3)}S_1+\beta_{33}^{\mathrm{sr}}D_3, \tag{2c}$$

where T_1 and T_2 are the radial and circumferential stresses, respectively, of piezoelectric elements; S_1 and S_2 are the radial and circumferential strains, respectively, of piezoelectric elements; D_3 and E_3 are the electric displacement and electric field, respectively; s_{11} is the compliance at constant electric field, g_{31} is the piezoelectric coefficient; $\beta_{33}^{\mathrm{sr}}=1/[(\varepsilon_{33}^{\mathrm{T}})^{(1-\kappa_{\mathrm{p}}^2)}]$, where $\varepsilon_{33}^{\mathrm{T}}$ is the permittivity at constant stress of the piezoelectric layers, κ_{p} is the electromechanical coupling coefficient; σ_3 is the Poisson ratio of the piezoelectric element.

In thermodynamic equilibrium, the strain energy density of an infinitesimally small volume element in piezoelectric materials D_{p} is given by

$$D_{\mathrm{p}}=T_1S_1/2+T_2S_2/2. \tag{3}$$

By substitution of Eq.(2) into Eq.(3), we obtain

$$D_{\mathrm{p}}=\frac{S_1^2+S_2^2+2\sigma_3S_1S_2}{2s_{11}(1-\sigma_3^2)}-\frac{g_{31}(S_1+S_2)}{2s_{11}(1-\sigma_3^2)}D_3. \tag{4}$$

With the relationship between the strain and the curvature of the mid-plane, we get

$$\begin{cases}S_1=z\mu_1,\\ S_2=z\mu_2,\end{cases} \tag{5}$$

where z is the distance from the natural surface, and μ_1 and μ_2 are the curvatures of mid-plane.

By substitution of Eq.(5) into Eq.(4), the unit area of the strain energy in the piezoelectric element can be obtained by a thickness direction integration:

$$u_{\mathrm{p}}=\int_z D\mathrm{d}z=\frac{(t_3^2-t_2^2)(\mu_1^2+\mu_2^2+2\sigma_3\mu_1\mu_2)}{24s_{11}(1-\sigma_3^2)}-\frac{(t_3^2-t_2^2)g_{31}(\mu_1+\mu_2)}{8s_{11}(1-\sigma_3)}D_3. \tag{6}$$

By Eq.(2c), the voltage of the electric field can be obtained:

$$V=\int_z E_3\mathrm{d}z=\frac{(t_3^2-t_2^2)g_{31}(\mu_1+\mu_2)}{8s_{11}(1-\sigma_3)}-\frac{(t_3-t_2)}{2}\beta_{33}^{\mathrm{sr}}D_3. \tag{7}$$

Therefore, we have

$$D_3=\frac{(t_3+t_2)(\mu_1+\mu_2)g_{31}}{4s_{11}(1-\sigma_3)\beta_{33}^{\mathrm{sr}}}-\frac{2V}{(t_3-t_2)\beta_{33}^{\mathrm{sr}}}. \tag{8}$$

By substitution of Eq.(8) into Eq.(6), the unit area of the strain energy can be calculated as

$$u_{\mathrm{p}}=\frac{(t_3^3-t_2^3)}{24s_{11}(1-\sigma_3^2)}[(\mu_1+\mu_2)^2-2(1-\sigma_3)\mu_1\mu_2]-\frac{(t_3^2-t_2^2)(t_3+t_2)\kappa_{\mathrm{p}}^2}{64s_{11}(1-\sigma_3)}(\mu_1+\mu_2)^2+\frac{(t_3+t_2)(\mu_1+\mu_2)g_{31}V}{4s_{11}(1-\sigma_3)\beta_{33}^{\mathrm{sr}}}. \tag{9}$$

For the elastic layer element, we can obtain:

$$\begin{cases}T_1'=-\dfrac{Ez}{1-\sigma_{\mathrm{m}}^2}(\mu_1+\sigma_{\mathrm{m}}\mu_2),\\ T_2'=-\dfrac{Ez}{1-\sigma_{\mathrm{m}}^2}(\sigma_{\mathrm{m}}\mu_1+\mu_2),\end{cases} \tag{10}$$

where T_1' and T_2' are the radial and circumferential stresses, respectively, and σ_{m} and E are the Poisson ratio and elastic modulus, respectively, of the metal element.

By Eqs.(3), (5) and (10), the strain energy density of an infinitesimally small volume element in the brass disk where $r\leq r_3$ can be obtained:

$$D_{\mathrm{b}}=\frac{E_2z^3}{2(1-\sigma_2^2)}(\mu_1^2+2\sigma_2\mu_1\mu_2+\mu_2^2), \tag{11}$$

where E_2 and σ_2 are the elastic modulus and Poisson ratio, respectively, of the brass disk.

Therefore, the unit area of the strain energy in the brass disk where $r\leq r_3$ can be calculated as

$$u_{\mathrm{b}}=\int_z D_{\mathrm{b}}\mathrm{d}z=\frac{(t_2^3-t_1^3)}{24s_{11}(1-\sigma_2^2)}[(\mu_1+\mu_2)^2-2(1-\sigma_2)\mu_1\mu_2]. \tag{12}$$

From Eqs.(9) and (12), the total strain energy of the PZT and brass composite disk where $r\leq r_3$ can be obtained by an area integration:

$$\begin{aligned}U_1&=\iint_s(u_{\mathrm{p}}+u_{\mathrm{b}})\mathrm{d}s\\&=\pi D_{\mathrm{c}}\int_0^{r_3}[(\mu_1+\mu_2)^2-2(1-\sigma_{\mathrm{c}})\mu_1\mu_2+\tau V(\mu_1+\mu_2)]r\mathrm{d}r,\end{aligned} \tag{13}$$

where D_{c} and σ_{c} are the effective bending stiffness and Poisson ratio of the PZT and brass composite disk, respectively, and

$$D_{\mathrm{c}}=\frac{t_3^3-t_2^3}{12s_{11}(1-\sigma_3^2)}+\frac{E_2(t_3^3-t_2^3)}{12s_{11}(1-\sigma_2^2)}-\frac{\kappa_{\mathrm{p}}^2(t_3^2-t_2^2)(t_3+t_2)}{32s_{11}(1-\sigma_3^2)},$$

$$2(1-\sigma_{\mathrm{c}})=\frac{1}{D_{\mathrm{c}}}\left[\frac{t_3^3-t_2^3}{6s_{11}(1+\sigma_3)}+\frac{E_2(t_2^3-t_1^3)}{6(1+\sigma_2)}\right],$$

$$\tau=\frac{(t_3+t_2)g_{31}}{2s_{11}(1-\sigma_3)\beta_{33}^{\mathrm{sr}}D_{\mathrm{c}}}.$$

Similarly, the strain energy of the brass ring U_2 where $r_3<r\leq r_2$, and the steel ring U_3 where $r_1<r\leq r_2$ can be obtained as follows:

$$U_2=\pi D_{\mathrm{m}}\int_{r_3}^{r_2}[(\mu_1+\mu_2)^2-2(1-\sigma_2)\mu_1\mu_2]r\mathrm{d}r, \tag{14}$$

$$U_3=\pi D'_{\mathrm{m}}\int_{r_3}^{r_2}[(\mu_1+\mu_2)^2-2(1-\sigma_1)\mu_1\mu_2]r\mathrm{d}r, \tag{15}$$

where D_{m} and D'_{m} are the effective bending stiffness of the brass ring and steel ring, respectively, $D_{\mathrm{m}}=\dfrac{\pi E_2(t_2^3-t_1^3)}{12(1-\sigma_2^2)}$, $D'_{\mathrm{m}}=\dfrac{\pi E_1t_1^3}{12(1-\sigma_1^2)}$, and E_1 and σ_1 are the elastic modulus and Poisson ratio, respectively, of the steel ring.

From Eqs.(13)~(15), the total strain energy of the drum transducer can be obtained:

$$U_{\max}=U_1+U_2+U_3. \tag{16}$$

The kinetic energy of the drum transducer can be denoted as

$$T=\frac{1}{2}\rho h\iint_s\left(\frac{\partial w}{\partial t}\right)^2 r\mathrm{d}s=\rho\pi h\int_r\left(\frac{\partial w}{\partial t}\right)^2 r\mathrm{d}r. \quad (17)$$

Therefore, the total kinetic energy of the drum transducer can be calculated as

$$\begin{aligned}T=&\rho_1\pi t_1\omega^2\int_{r_1}^{r_2}w_1^2 r\mathrm{d}r+\rho_2\pi(t_2-t_1)\omega^2\int_{r_3}^{r_2}w_1^2 r\mathrm{d}r\\&+\rho_2\pi(t_2-t_1)\omega^2\int_0^{r_3}w_3^2 r\mathrm{d}r+\rho_3\pi(t_3-t_2)\omega^2\int_0^{r_3}w_3^2 r\mathrm{d}r,\end{aligned} \quad (18)$$

where ω is the frequency of active force; ρ_1, ρ_2 and ρ_3 are the densities of steel ring, brass and PZT, respectively; w_1, w_2 and w_3 are the vertical displacements of the steel ring, brass and ceramic-metal disks, respectively.

The electric energy of the drum transducer can be given as

$$\begin{aligned}U^{\mathrm{E}}&=\iiint_V E_3D_3r\mathrm{d}V=\int_0^{2\pi}\int_{t_2}^{t_3}\int_0^{r_3}E_3D_3r\mathrm{d}\theta\mathrm{d}z\mathrm{d}r\\&=-\pi D_{\mathrm{c}}\tau V\int_0^{r_3}(\mu_1+\mu_2)r\mathrm{d}r+\frac{2\pi r_3^2V^2}{(t_3-t_2)\beta_{33}^{\mathrm{sr}}}.\end{aligned} \quad (19)$$

Therefore, the maximal electric energy of the drum transducer can be expressed as

$$U_{\max}^{\mathrm{E}}=\pi D_{\mathrm{c}}\int_0^{r_3}\tau V(\mu_1+\mu_2)r\mathrm{d}r+\frac{2\pi r_3^2V^2}{(t_3-t_2)\beta_{33}^{\mathrm{sr}}}. \quad (20)$$

The curvature of the mid-plane is defined as (Liu *et al*., 2002)

$$\begin{cases}\mu_1=-\dfrac{\partial^2 w}{\partial r^2},\\[2mm]\mu_2=-\dfrac{1}{r}\dfrac{\partial w}{\partial r}.\end{cases} \quad (21)$$

Based on the Rayleigh-Ritz method and the symmetrical structure, the functional analysis of the drum transducer can be given as

$$L=U_{\max}-T_{\max}-U_{\max}^{\mathrm{E}}, \quad (22)$$

where $U_{\max}$, $T_{\max}$ and $U_{\max}^{\mathrm{E}}$ are the maximal strain energy, kinetic energy and electric energy, respectively, of the drum transducer.

By substitution of Eqs.(16), (18), (20) and (21) into Eq.(22), we have

$$\begin{aligned}L=&\pi D_{\mathrm{c}}\int_0^{r_3}\left[\left(\frac{\partial^2 w_3}{\partial r^2}+\frac{1}{r}\frac{\partial w_3}{\partial r}\right)^2-2(1-\sigma_{\mathrm{c}})\frac{\partial^2 w_3}{\partial r^2}\frac{1}{r}\frac{\partial w_3}{\partial r}\right.\\&\left.-\tau V\left(\frac{\partial^2 w_3}{\partial r^2}+\frac{1}{r}\frac{\partial w_3}{\partial r}\right)\right]r\mathrm{d}r+\pi D_{\mathrm{m}}\int_{r_3}^{r_2}\left[\left(\frac{\partial^2 w_2}{\partial r^2}+\frac{1}{r}\frac{\partial w_2}{\partial r}\right)^2\right.\\&\left.-2(1-\sigma_2)\frac{\partial^2 w_2}{\partial r^2}\frac{1}{r}\frac{\partial w_2}{\partial r}\right]r\mathrm{d}r+\pi D'_{\mathrm{m}}\int_{r_1}^{r_2}\left[\left(\frac{\partial^2 w_1}{\partial r^2}+\frac{1}{r}\frac{\partial w_1}{\partial r}\right)^2\right.\\&\left.-2(1-\sigma_1)\frac{\partial^2 w_1}{\partial r^2}\frac{1}{r}\frac{\partial w_1}{\partial r}\right]r\mathrm{d}r-\rho_1\pi t_1\omega^2\int_{r_1}^{r_2}w_1^2 r\mathrm{d}r\\&-\rho_2\pi(t_2-t_1)\omega^2\int_{r_3}^{r_2}w_2^2 r\mathrm{d}r-\rho_2\pi(t_2-t_1)\omega^2\int_0^{r_3}w_3^2 r\mathrm{d}r\\&-\rho_3\pi(t_3-t_2)\omega^2\int_0^{r_3}w_3^2 r\mathrm{d}r\\&-\pi D_{\mathrm{c}}\int_0^{r_3}\tau V\left(\frac{\partial^2 w_3}{\partial r^2}+\frac{1}{r}\frac{\partial w_3}{\partial r}\right)r\mathrm{d}r-\frac{2\pi r_3^2V^2}{(t_3-t_2)\beta_{33}^{\mathrm{sr}}},\end{aligned} \quad (23)$$

where $V=-\dfrac{(t_3^2-t_2^2)g_{31}}{4s_{11}(1-\sigma_3)r_3^2}\left[r\dfrac{\mathrm{d}w_3}{\mathrm{d}r}\right]\Big|_0^{r_3}$.

When the drum transducer has a clamped support at the edge of the steel cylinder, the boundary condition can be described as

$$\begin{cases}w_2=0,\\[2mm]\dfrac{\mathrm{d}w_2}{\mathrm{d}r}=0,\end{cases} \quad (24)$$

where $r=r_2$.

The approximate function of vertical displacement can be written as

$$w=A(r_2^2-r^2)^2. \quad (25)$$

Similarly, by substitution of Eq.(25) into Eq.(23), and $\dfrac{\mathrm{d}L}{\mathrm{d}A}=0$, we have

$$A=F\varphi_9/(2\pi H). \quad (26)$$

By H=0 (refer to Section APPENDIX), the first resonance frequency equation of a drum transducer with a clamped support can be given as

$$\omega^2=\frac{D_c\left[\varphi_1-2(1-\sigma_c)\varphi_2-\dfrac{4\tau(t_3^2-t_2^2)g_{31}}{s_{11}(1-\sigma_3)}\varphi_2\right]+D_m[\varphi_3+2(1-\sigma_2)\varphi_2]+D'_m[\varphi_4+2(1-\sigma_1)\varphi_2]}{4r_2^4\rho_1(t_1+t_2)\varphi_5+r_2^4\rho_1t_1\varphi_6+r_2^4\rho_2(t_2-t_1)\varphi_7+r_2^4[\rho_2(t_2-t_1)+\rho_3(t_3-t_2)]\varphi_8}. \quad (27)$$

FINITE ELEMENT ANALYSIS

FEM is the most powerful tool available today in designing composite transducers. It can handle complex structures with irregular boundaries (Duan *et al*., 2005; Li *et al*., 2007). Modal analysis calculates the resonance frequencies and the corresponding deformation shape of the structure. Here, the function of the PZT is electrostatic-structural conversion. Therefore, the finite element SOLID 227 was chosen for the element of PZT that supports the coupled-field (Frangi *et al*., 2005). The drum transducer model was established and the edge of the drum transducer was fixed. Table 1 gives the material properties and structural parameters of the drum transducer analyzed in this study. The other PZT5H parameters (Auld, 1973) are given below as: c_{11}=12.6 N/m^2, c_{33}=11.7 N/m^2, c_{44}=2.30 N/m^2, c_{12}=7.95 N/m^2, c_{13}=8.41 N/m^2, e_{15}=17.0 C/m^2, e_{31}=−6.5 C/m^2, e_{33}=23.3 C/m^2, ε_{11}=1700ε_0, ε_{33}=1470ε_0, ε_0=8.854×10^{-12} F/m, where c_{ij}, e_{ij} and ε_{ij} are the elastic, piezoelectric and dielectric constants, respectively, where i, j (i, j=1, 2, 3, 4, 5, 6) denote tensor notation.

Table 1 Material properties and structural parameters of the drum transducer

Parameter	PZT5H	Steel	Brass
Density (kg/m^3)	7600	7800	8920
Elastic modulus (GPa)	76.5	200	117
Poisson ratio	0.36	0.29	0.35
d_1 (mm)		8.6	
d_2 (mm)		20	20
d_3 (mm)	16		
t_1 (mm)		0.8	
t_2 (mm)			1.2
t_3 (mm)	1.4		

Fig.2 shows the first resonance vibration mode of a drum transducer with a clamped support, at a first resonance frequency of 22.764 kHz.

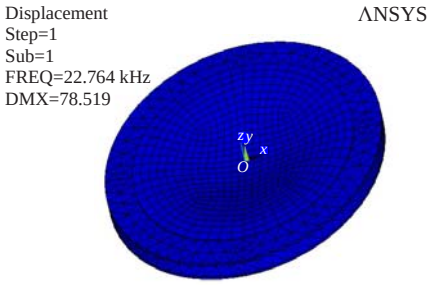

Fig.2 First resonance vibration mode of the drum transducer

EXPERIMENTAL MEASUREMENTS AND RESULTS

A drum transducer was fabricated, and its structural parameters are shown in Table 1. The resonance frequency of the drum transducer was measured using an impedance analyzer (4294 A, Agilent Inc.). Fig.3 shows the results in which curves A and B illustrate the impedance and phase variation, respectively. The frequencies of the theoretical analysis, FEM and experimental results are 22.58, 22.76, and 22.36 KHz, respectively. The results of the theoretical analysis were in good agreement with those of FEM and experimental results. The differences between theoretical analysis, FEM and measured results are mainly caused by the FEM simulation errors, including the inaccuracy of the real and simulated material property parameters, the neglect of the epoxide resin, etc. (Li *et al*., 2007).

As reported in previous investigations, the inner diameter is an important design parameter for enhancing the performance of a transducer (Sun *et al*., 2007). Fig.4 shows the results obtained from theoretical analysis and from FEM with different inner diameters. It can be seen that the numerical results are in good agreement with those obtained by FEM and that the resonance frequency of the drum transducer decreases as the inner diameter increases.

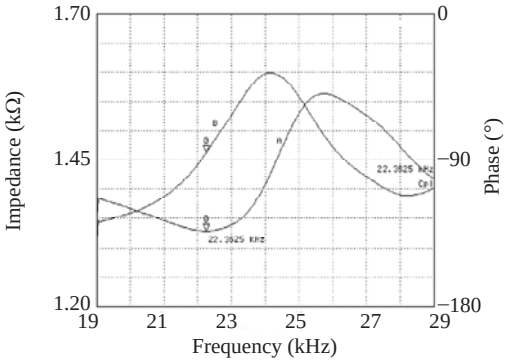

Fig.3 First resonance frequency of the drum transducer

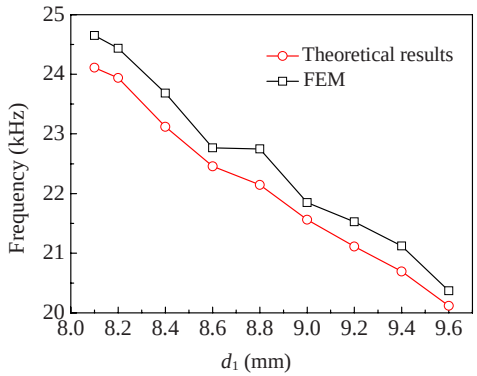

Fig.4 Frequency-inner diameter curves of the drum transducer

CONCLUSION

Based on thin plate elastic theory of piezoelectric and metal material combined with the Rayleigh-Ritz method, an equation for the calculation of the resonance frequency of a drum transducer was obtained. The results obtained from theoretical analysis were in very good agreement with those from FEM and experimental results. An excellent consistency was found between the theoretical results and those obtained by FEM with different inner diameters. The results showed that the resonance frequency of the drum decreases as its inner diameter increases.

References

Auld, B.A., 1973. Acoustic Fields and Waves in Solids. Wiley, New York, p.357-382.

Chen, W.S., Shi, S.J., 2007. A bidirectional standing wave ultrasonics linear motor based on langevin bending transducer. *Ferroelectrics*, **350**(5):102-110. [doi:10.1080/00150190701369958]

Cornwell, P.J., Goethal, J., Kowko, J., Damianakis, M., 2005. Enhancing power harvesting using a tuned auxiliary structure. *Journal of Intelligent Material Systems and Structures*, **16**(10):825-834. [doi:10.1177/1045389X05055279]

Duan, W.H., Quek, S.T., Lim, S.P., 2005. Finite Element Analysis of a Ring Type Ultrasonic Motor. Proceedings of SPIE, p.575-586. [doi:10.1117/12.597983]

Frangi, A., Corigliano, A., Binci, M., Faure, P., 2005. Finite element modelling of a rotating piezoelectric ultrasonic motor. *Ultrasonics*, **43**(9):747-755. [doi:10.1016/j.ultras.2005.04.005]

Hao, M., Chen, W.S., 2006. Analysis and Design Ring-type Traveling Wave Ultrasonic Motor. Proceedings of the IEEE International Conference Mechatronics and Automation, Luoyang, p.1806-1810. [doi:10.1109/ICMA.2006.257508]

Kim, H.W., Priya, S., Ken, J.U., 2006. Modeling of piezoelectric energy harvesting using cymbal transducers. *Japanese Journal of Applied Physics*, **45**(7):5836-5840. [doi:10.1143/JJAP.45.5836]

Kim, H.W., Priya, S., Stephanou, H., Uchino, K.J., 2007. Consideration of impedance matching techniques for efficient piezoelectric energy harvesting. *IEEE Transactions on Ultrasonics, Ferroelectrics, and Frequency Control*, **54**(9):1851-1859. [doi:10.1109/TUFFC.2007.469]

Li, X., Chen, W.S., Xie, T., Liu, J.K., 2007. Novel high torque bearingless two-sided rotary ultrasonic motor. *Journal of Zhejiang University SCIENCE A*, **8**(5):786-792. [doi:10.1631/jzus.2007.A0786]

Liu, P.K., Sun, L.N., Zhu, Y.H., Zhao, Y.F., 2002. Analysis on piezoelectric bimorph actuator for In-pipe Micro Robot. *Piezoelectric & Acoustooptics*, **24**(2):111-115 (in Chinese).

Mateu, L., Moll, F., 2005. Optimum piezoelectric bending beam structures for energy harvesting using shoe inserts. *Journal of Intelligent Material Systems and Structures*, **16**(10):835-845. [doi:10.1177/1045389X05055280]

Mateu, L., Moll, F., 2007. System-level Simulation of a Self-powered Sensor with Piezoelectric Energy Harvesting. International Conference on Sensor Technologies and Applications, **16**(10):399-404. [doi:10.1109/SENSORCOMM.2007.4394954]

Sun, C.L., Lam, K.H., Chan, H.L.W., Choy, C.L., 2006. A novel drum piezoelectric-actuator. *Applied Physics A*, **84**(4):385-389. [doi:10.1007/s00339-006-3641-x]

Sun, C.L., Lam, K.H., Lu, S.G., Chan, H.L.W., Zhao, X.Z., Choy, C.L., 2007. Effect of geometry on the characteristics of a drum actuator. *Journal of Intelligent Material Systems and Structures*, **18**:1-6. [doi:10.1177/1045389X06072362]

Uchino, K., 1999. Recent Trend of Piezoelectric Actuator Developments. Micromechatronics and Human Science, Nagoya, Japan, p.3-9. [doi:10.1109/MHS.1999.819975]

Wang, S., Kwok, H.L., Sun, C.L., Kin, K.W., Chan, H.L.W., Ming, S.G., Xing, Z.Z., 2007. Energy harvesting with

piezoelectric drum transducer. *Applied Physics Letters*, **90**(11):113506-113508. [doi:10.1063/1.2713357]

APPENDIX

$$
\begin{aligned}
H = {} & D_c r_2^2 \left[\varphi_1 - 2(1-\sigma_c)\varphi_2 - \frac{4\tau(t_3^2 - t_2^2) g_{31}}{s_{11}(1-\sigma_3)} \varphi_2 \right] \\
& + D_m r_2^2 [\varphi_3 + 2(1-\sigma_2)\varphi_2] + D'_m r_2^2 [\varphi_4 + 2(1-\sigma_1)\varphi_2] \\
& - \omega^2 r_2^6 \rho_1 t_1 \varphi_6 - \omega^2 r_2^6 \rho_2 (t_2 - t_1)\varphi_7 \\
& - \omega^2 r_2^6 [\rho_2 (t_2 - t_1) + \rho_3 (t_3 - t_2)]\varphi_8,
\end{aligned}
$$

where

$$
\begin{aligned}
& \varphi_1 = 32(4\beta_2^6 - 6\beta_2^4 + 3\beta_2^2)/3, \\
& \varphi_2 = 8\beta_2^2 (1-\beta_2^2)^2, \\
& \varphi_3 = 32(1 - 3\beta_2^2 + 6\beta_2^4 - 4\beta_2^6)/3, \\
& \varphi_4 = 32(4 - 3\beta_2^2 + 6\beta_2^4 - 4\beta_2^6)/3, \\
& \varphi_5 = 8\beta_1^2 (1-\beta_1^2)^2, \ \varphi_6 = (1-\beta_1^2)^5/10, \\
& \varphi_7 = (1-\beta_2^2)^5/10, \ \varphi_8 = [1-(1-\beta_2^2)^5]/10, \\
& \varphi_9 = -\beta_1^4 + 2\beta_1^2 - 2, \ \beta_1 = r_1/r_2, \ \beta_2 = r_3/r_2.
\end{aligned}
$$